Self-Consistent Kinetic Description of the Longitudinal Dynamics of Intense Charged Particle Beams.*

R. C. Davidson, E. A. Startsev and H. Qin
Plasma Physics Laboratory, Princeton University
Princeton, New Jersey, 08543, USA

2010 International Symposium on Heavy Ion Fusion
August 30–September 3, 2010
University of Darmstadt
Darmstadt, Germany

*Research supported by the U.S. Department of Energy.

Abstract

A self-consistent kinetic model is developed that describes the longitudinal dynamics of a long, coasting beam propagating in straight (linear) geometry in the z-direction in the smooth-focusing approximation. Making use of the three-dimensional Vlasov-Maxwell equations, and integrating over the phase space $(\mathbf{x}_\perp, \mathbf{p}_\perp)$ transverse to beam propagation, a closed system of equations is obtained for the nonlinear evolution of the longitudinal distribution function $F_b(z, p_z, t)$ and average axial electric field $\langle E_z^s \rangle(z,t)$. The primary assumptions in the present analysis are that the dependence on axial momentum p_z of the distribution function $f_b(\mathbf{x}, \mathbf{p}, t)$ is factorable, and that the transverse beam dynamics remains relatively quiescent (absence of transverse instability or beam mismatch). The analysis is carried out correct to order $k_z^2 r_w^2$ assuming slow axial spatial variations with $k_z^2 r_w^2 \ll 1$, where $k_z \sim \partial/\partial z$ is the inverse length scale of axial variation in the line density, and r_w is the radius of the conducting wall (assumed perfectly conducting). A closed expression for the average longitudinal electric field $\langle E_z^s \rangle(z,t)$, expressed in terms of geometric factors, the line density λ_b, and its derivatives $\partial\lambda_b/\partial z, \cdots$, is presented for the class of bell-shaped density profiles $n_b(r,z,t) = (\lambda_b/\pi r_b^2) f(r/r_b)$, where $f(r/r_b)$ is the density shape function, and r_b is the beam edge radius. The general formalism described in this paper is valid for the entire range of beam intensities (proportional to λ_b) ranging from low-intensity, emittance-dominated beams, to very-high-intensity, low-emittance beams. The properties of the solitary-wave structures are also investigated.

Theoretical Model and Assumptions

- Long coasting beam propagating in z-direction through perfectly conducting cylinder with wall radius located at $r = r_w$.

- The nonlinear Vlasov-Maxwell equations in the beam frame describing the self-consistent nonlinear evolution of $f_b(\mathbf{x}, \mathbf{p}, t)$ and $\mathbf{E}^s(\mathbf{x}, t)$ can be expressed as

$$\frac{\partial f_b}{\partial t} + \mathbf{v} \cdot \frac{\partial f_b}{\partial \mathbf{x}} + (\mathbf{F}^{tr}_{foc} + e_b \mathbf{E}^s) \cdot \frac{\partial f_b}{\partial \mathbf{p}} = 0,$$

  and

$$\nabla \cdot \mathbf{E}^s = 4\pi e_b \int d^3p f_b, \quad \nabla \times \mathbf{E}^s = 0,$$

  where $\mathbf{v} = \mathbf{p}/m_b$ is the (nonrelativistic) particle velocity in the beam frame.

Theoretical Model and Assumptions

- Two macroscopic moments of particular interest for a coasting beam (long charge bunch) are the volume number density $n_b(x, y, z, t)$ and axial line density $\lambda_b(z, t)$ defined by

$$\begin{aligned} n_b(\mathbf{x}, t) &= \int d^3p f_b(\mathbf{x}, \mathbf{p}, t) \ , \\ \lambda_b(z, t) &= \int dxdy n_b(\mathbf{x}, t) = \int dxdy \int d^3p f_b. \end{aligned}$$

  Here, $\int dxdy \cdots = \int_0^{r_w} drr \int_0^{2\pi} d\theta \cdots$ denotes integration over the accessible transverse configuration space.

- The nonlinear evolution of $f_b(\mathbf{x}, \mathbf{p}, t)$ is determined from

$$\frac{\partial}{\partial t} f_b + v_z \frac{\partial}{\partial z} f_b + \mathbf{v}_\perp \cdot \frac{\partial}{\partial \mathbf{x}_\perp} f_b + (\mathbf{F}^{tr}_{foc} + e_b \mathbf{E}_\perp) \cdot \frac{\partial}{\partial \mathbf{p}_\perp} f_b + e_b E^s_z \frac{\partial}{\partial p_z} f_b = 0.$$

  Here, $\mathbf{x}_\perp = x\hat{\mathbf{e}}_x + y\hat{\mathbf{e}}_y$ and $\mathbf{p}_\perp = p_x\hat{\mathbf{e}}_x + p_y\hat{\mathbf{e}}_y$ denote the transverse phase space variables, and $\mathbf{v}_\perp = \mathbf{p}_\perp / m_b$ is the transverse particle velocity.

Theoretical Model and Assumptions

- We introduce the transverse projection operator $\langle \cdots \rangle_\perp$ defined by

$$\langle \cdots \rangle_\perp = \int dxdy \int dp_x dp_y \cdots,$$

and the longitudinal distrbution function $F_b(z, p_z, t)$ defined by

$$F_b(z, p_z, t) = \langle f_b(\mathbf{x}, \mathbf{p}, t) \rangle_\perp = \int dxdy \int dp_x dp_y f_b(\mathbf{x}, \mathbf{p}, t),$$

- Some straightforward integration by parts then gives for the nonlinear evolution of $F_b(z, p_z, t)$

$$\frac{\partial}{\partial t} F_b + v_z \frac{\partial}{\partial z} F_b + e_b \langle E_z^s \frac{\partial}{\partial p_z} f_b \rangle_\perp = 0.$$

Theoretical Model and Assumptions

- For $\nabla \times \mathbf{E}^s \simeq 0$, it follows that $\partial E_z^s/\partial r = \partial E_r^s/\partial z$ and $\partial E_\theta^s/\partial z = r^{-1}\partial E_z^s/\partial \theta$. Poisson's equation for $E_z^s(r,\theta,z,t)$ readily becomes

$$\frac{1}{r}\frac{\partial}{\partial r}r\frac{\partial}{\partial r}E_z^s + \frac{\partial^2}{\partial z^2}E_z^s + \frac{1}{r^2}\frac{\partial^2}{\partial \theta^2}E_z^s = 4\pi e_b \frac{\partial}{\partial z}n_b,$$

  where $n_b(r,\theta,z,t) = \int d^3p f_b(r,\theta,z,\mathbf{p},t)$ is the number density of beam particles. Note that $\lambda_b(z,t) = \int dxdy n_b = \int dxdy \int d^3p f_b$ is related to the longitudinal distribution function $F_b(z,p_z,t)$ by

$$\lambda_b(z,t) = \int dp_z F_b(z,p_z,t).$$

- As a simplifying ansatz for closure, consistent with the assumption that the transverse beam dynamics remains relatively quiescent, we make the assumption that the dependence of $f_b(\mathbf{x},\mathbf{p},t)$ on axial momentum p_z is factorable according to

$$f_b(\mathbf{x},\mathbf{p},t) = G_b(\mathbf{x}_\perp,\mathbf{p}_\perp,z,t)F_b(z,p_z,t),$$

  where $G_b(\mathbf{x}_\perp,\mathbf{p}_\perp,z,t)$ and $F_b(z,p_z,t)$ are the transverse and longitudinal distribution functions.

Theoretical Model and Assumptions

- These assumptions and definitions readily give

$$\int dp_x dp_y G_b(\mathbf{x}_\perp, \mathbf{p}_\perp, z, t) = \frac{n_b(\mathbf{x}, t)}{\lambda_b(z, t)}.$$

$$e_b \langle E_z^s \frac{\partial}{\partial p_z} f_b \rangle_\perp = e_b \langle E_z^s \rangle (z, t) \frac{\partial}{\partial p_z} F_b(z, p_z, t),$$

where the average axial electric field $\langle E_z \rangle (z, t)$ is defined by

$$\langle E_z^s \rangle (z, t) \equiv \langle E_z^s(\mathbf{x}, t) G_b(\mathbf{x}_\perp, \mathbf{p}_\perp, z, t) \rangle_\perp = \int dx dy E_z(\mathbf{x}, t) \frac{n_b(\mathbf{x}, t)}{\lambda_b(z, t)}.$$

Theoretical Model and Assumptions

- The final set of equations describing the nonlinear evolution of $F_b(z, p_z, t)$ and $\langle E_z^s \rangle(z, t)$ are given by

$$\frac{\partial}{\partial t} F_b + v_z \frac{\partial}{\partial z} F_b + e_b \langle E_z^s \rangle \frac{\partial}{\partial p_z} F_b = 0,$$

and

$$\langle E_z^s \rangle = 2\pi \int_0^{r_w} dr r \frac{n_b(r, z, t)}{\lambda_b(z, t)} E_z^s(r, z, t).$$

- Here, $E_z^s(r, z, t)$ is determined self-consistently in terms of the density profile $n_b(r, z, t)$ from Poisson's equation, which can be expressed as

$$\frac{1}{r} \frac{\partial}{\partial r} r \frac{\partial}{\partial r} E_z^s + \frac{\partial^2}{\partial z^2} E_z^s = 4\pi e_b \frac{\partial}{\partial z} n_b$$

for $\partial/\partial\theta = 0$. In addition, the line density $\lambda_b(z, t)$ is related to $F_b(z, p_z, t)$ and $n_b(r, z, t)$ by

$$\lambda_b(z, t) = 2\pi \int_0^{r_w} dr r n_b(r, z, t) = \int dp_z F_b(z, p_z, t).$$

Theoretical Model and Assumptions

- For our purposes here, we specialize to the case where the z-variation in $E_z^s(r,z,t)$ is slow in comparison with the r-variation. In particular, denoting $\partial/\partial z \sim L_z^{-1} \sim k_z$, it is assumed that

$$k_z^2 r_w^2 \ll 1,$$

where r_w is the conducting wall radius.

- Imposing the boundary condition $E_z^s(r = r_w, z, t) = 0$ at the perfecting conducting wall, the formal solution can be expressed as

$$E_z^s(r,z,t) = -4\pi e_b \int_r^{r_w} \frac{dr}{r} \int_0^r drr\left(\frac{\partial n_b}{\partial z} - \frac{1}{4\pi e_b}\frac{\partial^2 E_z^2}{\partial z^2}\right),$$

where $n_b(r,z,t)$ is the density profile. The second term on the right-hand side is small in comparison with the first term. Solving iteratively for $E_z^s(r,z,t)$ then gives

$$E_z^s(r,z,t) = -4\pi e_b \int_r^{r_w} \frac{dr}{r} \int_0^r drr\left(\frac{\partial n_b}{\partial z} + \int_r^{r_w} \frac{dr}{r} \int_0^r drr\frac{\partial^3 n_b}{\partial z^3}\right)$$

correct to $0(k_z^2 r_w^2)$.

Evaluation of Average Longitudinal Electric Field

- The average electric field $\langle E_z^s \rangle(z,t) = \int dxdy E_z(\mathbf{x},t)\frac{n_b(\mathbf{x},t)}{\lambda_b(z,t)}$ can then be expressed as

$$\langle E_z^s \rangle = \langle E_z^s \rangle^{(1)} + \langle E_z^s \rangle^{(2)},$$

where $\langle E_z^s \rangle^{(1)}$ and $\langle E_z^s \rangle^{(2)}$ are defined by

$$\langle E_z^s \rangle^{(1)} = -2e_b \int_0^{r_w} \frac{dr}{r}\Big(2\pi \int_0^r drr\frac{n_b}{\lambda_b}\Big)\frac{\partial}{\partial z}\Big(2\pi \int_0^r drr\frac{n_b}{\lambda_b}\cdot\lambda_b\Big),$$

and

$$\langle E_z^s \rangle^{(2)} = -2e_b \int_0^{r_w} \frac{dr}{r}\Big(2\pi \int_0^r drr\frac{n_b}{\lambda_b}\Big)\frac{\partial^3}{\partial z^3}\int_0^r drr\int_r^{r_w} \frac{dr}{r}\Big(2\pi \int_0^r drr\frac{n_b}{\lambda_b}\cdot\lambda_b\Big).$$

These equations can be used to evaluate a closed expression for $\langle E_z^s \rangle = \langle E_z^s \rangle^{(1)} + \langle E_z^s \rangle^{(2)}$ and the corresponding g-factors for a wide range of choices of beam density profiles $n_b(r,z,t)$.

Radial Force Balance

- For a broad range of choices of transverse quasi-equilibrium distributions $G_b(H_\perp)$, radial force balance for a matched beam can be expressed as

$$\omega_{\beta\perp}^2 R_b^2 = \lambda_b \frac{e_b^2}{m_b} + \frac{1}{4}\frac{\tilde{\epsilon}^2}{R_b^2}.$$

or equivalently,

$$R_b^4 - R_\lambda^2 R_b^2 - R_\epsilon^4 = 0,$$

where

$$R_\lambda^2 = \frac{\lambda_b e_b^2}{m_b \omega_{\beta\perp}^2}\ , \quad R_\epsilon^4 = \frac{\tilde{\epsilon}^2}{4\omega_{\beta\perp}^2}.$$

where $R_b^2 = \langle r^2 \rangle$ is the mean-square beam radius, and the scaled transverse emittance $\tilde{\epsilon}$ is defined by $\tilde{\epsilon}^2/4R_b^2 = \langle v_\perp^2 \rangle$.

Radial Force Balance

- The physically acceptable solutions for R_b^2 is given by

$$R_b^2 = \frac{1}{2}[R_\lambda^2 + (R_\lambda^4 + 4R_\epsilon^4)^{1/2}].$$

  Note that the mean-square beam radius R_b^2 depends on the line density λ_b.

- For a low-intensity emittance-dominated beam with $R_\lambda^2 \ll 2R_\epsilon^2$, R_b^2 reduces to the familiar result $R_b^2 \simeq R_\epsilon^2 = \tilde{\epsilon}/2\omega_{\beta\perp}$, which is independent of λ_b.

- On the other hand, for a very-low-emittance, space-charge-dominated beam with $R_\lambda^2 \gg 2R_\epsilon^2$, we obtain $R_b^2 \simeq R_\lambda^2 = \lambda_b e_b^2/m_b\omega_{\beta\perp}^2$, which is linearly proportional to the line density λ_b. A plot of R_b^2/R_ϵ^2 versus R_λ^2/R_ϵ^2 illustrating this behavior is shown in the figure.

Radial Force Balance

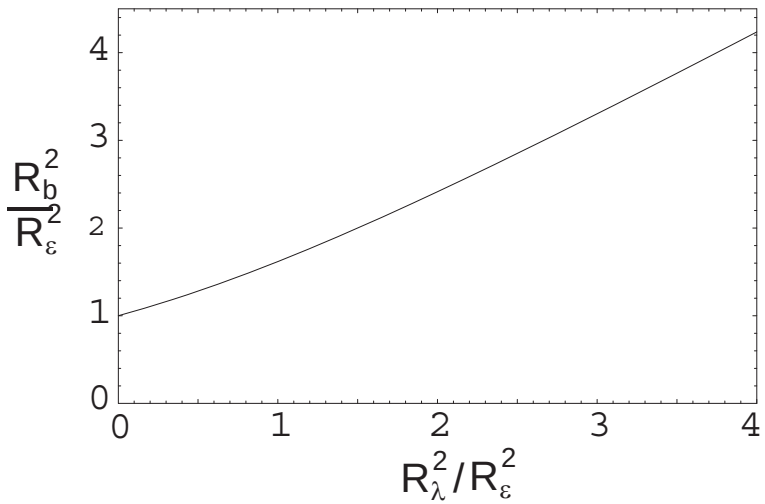

Plot of R_b^2/R_ϵ^2 versus R_λ^2/R_ϵ^2 obtained from the radial force balance equation.

Fixed-Shape Density Profile

- We specialize to the class of fixed-shape density profiles $n_b(r, z, t)$ of the form

$$n_b = \begin{cases} \dfrac{\lambda_b}{\pi r_b^2} f\left(\dfrac{r}{r_b}\right) \ , & 0 \le r < r_b \ , \\ 0 \ , & r_b < r \le r_w, \end{cases}$$

  where $f(r/r_b)$ is a smooth function that depends on the scaled radial variable r/r_b.

- From $\lambda_b = 2\pi \int_0^{r_w} dr r n_b$, we obtain the normalization condition

$$\int_0^1 dX X f(X) = \frac{1}{2}.$$

  Similarly, from $R_b^2 = \langle r^2 \rangle = (2\pi \int_0^{r_w} dr r r^2 n_b)/\lambda_b$, we obtain

$$R_b^2 = \eta_b r_b^2$$

  where the constant η_b is defined by

$$\eta_b = 2 \int_0^1 dX X X^2 f(X).$$

- For specified shape function $f(r/r_b)$ the edge radius r_b can be expressed as

$$r_b^2 = \frac{1}{2\eta_b}[R_\lambda^2 + (R_\lambda^4 + 4R_\epsilon^4)^{1/2}].$$

Fixed-Shape Density Profile

- One choice of shape profile of particular interest is

$$f_n\Big(\frac{r}{r_b}\Big) = (n+1)\Big[1 - \frac{r^2}{r_b^2}\Big]^n \ , \quad 0 \le r < r_b,$$

where $n = 0, 1, 2, \cdots$ is a positive integer. For this choice profile we readily obtain

$$\eta_b = \frac{1}{n+2}.$$

Here, the root-mean-square beam radius R_b is related to the edge radius r_b by $R_b^2 = \eta_b r_b^2$.

- The profile shape function $f(r/r_b)$ gives a wide range of density profile *peakedness*, ranging from a step-function density profile (for $n = 0$) to increasingly peaked profiles (for $n = 1, 2, \cdots$).

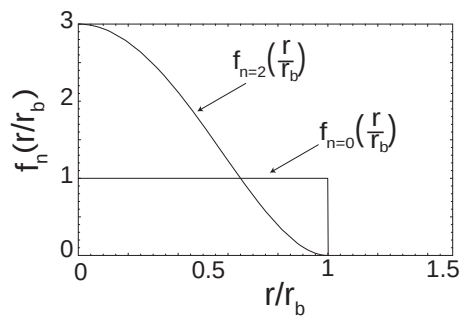

Shape function profile $f_n(r/r_b)$ plotted versus r/r_b for $n = 0$ and $n = 2$.

Evaluation of $\langle E_z^s \rangle^{(1)}$

- Because the beam edge radius r_b generally depends on the line density λ_b, it is clear that the radial integrations over n_b/λ_b required to evaluate $\langle E_z^s \rangle^{(1)}$ will also depend on λ_b.

- For the class of fixed-shape profiles considered here, some algebraic manipulation gives

$$\langle E_z^s \rangle^{(1)} = -e_b g_0(\lambda_b) \frac{\partial}{\partial z} \lambda_b(z,t)$$

where the $g_0(\lambda_b)$ is defined by

$$g_0(\lambda_b) = \ell n\left(\frac{r_w^2}{r_b^2}\right) + \alpha_n - \frac{1}{2} \frac{R_\lambda^2}{[R_\lambda^4 + 4R_\epsilon^4]^{1/2}}.$$

Here, $R_\lambda^2 = \lambda_b e_b^2 / m_b \omega_{\beta\perp}^2$ and $R_\epsilon^2 = \tilde{\epsilon}/2\omega_{\beta\perp}$, and

$$\alpha_n = \sum_{m=1}^{n+1} \frac{(n+1)}{m(m+n+1)}.$$

Evaluation of $\langle E_z^s \rangle^{(1)}$

- The expression for $g_0(\lambda_b)$ clearly displays the dependence of g_0 on the line density λ_b. For a low-intensity, emittance-dominated beam with $R_\lambda^2 \ll 2R_e^2$, the final term is approximately $-R_\lambda^2/4R_\epsilon^2$, which represents a negligibly small correction to $\ell n(r_w^2/r_b^2) + \alpha_n$.

- On the other hand, for a space-charge-dominated beam with $R_\lambda^2 \gg 2R_\epsilon^2$ the final term is approximately $-1/2$, representing a sizeable contribution to the g_0-factor. Indeed, for the special case of a step-function density profile ($n = 0$ and $\alpha_0 = 1/2$) the second and third terms on the right-hand side exactly cancel in the limit of a space-charge-dominated beam ($R_\lambda^2 \gg 2R_\epsilon^2$), and the g_0-factor is given approximately by $g_0 \simeq \ell n(r_w^2/r_b^2)$ as previously obtained by Reiser et al.

Evaluation of $\langle E_z^s \rangle^{(2)}$ for Low Beam Intensity

- The second-order electric field $\langle E_z^s \rangle^{(2)}$ is more difficult to calculate, even for the class of fixed-shape density profiles considered here. As a first example, we consider a low-intensity beam ($R_\lambda^2 \ll 2R_\epsilon^2$), and treat n_b/λ_b as independent of λ_b.

- In this case, we find

$$\langle E_z^s \rangle^{(2)} = -e_b g_2 r_w^2 \frac{\partial^3 \lambda_b}{\partial z^3},$$

where the g_2-factor is defined by

$$g_2 = \frac{1}{2}\Big[1 - (1-\beta_n)\frac{r_b^2}{r_w^2} - \frac{1}{n+2}\frac{r_b^2}{r_w^2}\ell n\Big(\frac{r_w^2}{r_b^2}\Big)\Big].$$

Here, the constant β_n is defined by

$$\beta_n = \frac{n+1}{n+2} - \sum_{m=1}^{n+1} \frac{1}{m(m+n+2)},$$

and r_b^2 is related to the mean-square radius R_b^2 by $R_b^2 = r_b^2/(n+2)$.

Evaluation of $\langle E_z^s \rangle^{(2)}$ for Low Beam Intensity

- It is clear that the value of the geometric factor g_2 exhibits a sensitive dependence on profile shape. For example, it follows that $\beta_0 = 1/6$ for a step-function density profile ($n = 0$), whereas $\beta_1 = 19/60$ for a parabolic density profile ($n = 1$). Furthermore, it follows that $g_2 > 0$, with $g_2 \simeq 1/2$ for $r_b^2/r_w^2 \ll 1$ and $g_2 \simeq (1/2)\beta_n$ for $r_b^2/r_w^2 \to 1$.

- For the special case of a step-function density profile ($n = 0$), note that the g_2-factor is given by

$$g_2 = \frac{1}{2}\left[1 - \frac{5}{6}\frac{r_b^2}{r_w^2} - \frac{1}{2}\frac{r_b^2}{r_w^2}\ell n\left(\frac{r_w^2}{r_b^2}\right)\right].$$

Evaluation of $\langle E_z^s \rangle^{(2)}$ for Step-Function Density Profile

- For arbitrary beam intensity, we specialize to the case of a step-function density profile ($n = 0$). Carrying out the integrations over r, we obtain

$$\begin{aligned}\langle E_z^s \rangle^{(2)} &= -\frac{1}{2} e_b r_w^2 \Big\{ \Big[1 - \frac{r_b^2}{r_w^2} - \frac{1}{2}\frac{r_b^2}{r_w^2} \ell n\Big(\frac{r_w^2}{r_b^2}\Big) \Big] \frac{\partial^3 \lambda_b}{\partial z^3} - \frac{1}{4} \ell n\Big(\frac{r_w^2}{r_b^2}\Big) \frac{\partial^3}{\partial z^3}\Big(\frac{\lambda_b r_b^2}{r_w^2}\Big) \\ &- \frac{1}{12}\frac{r_b^4}{r_w^4}\frac{\partial^3}{\partial z^3}\Big(\frac{\lambda_b r_w^2}{r_b^2}\Big) + \frac{1}{4}\frac{r_b^2}{r_w^2}\frac{\partial^3}{\partial z^3}\Big[\lambda_b \ell n\Big(\frac{r_w^2}{r_b^2}\Big) + \lambda_b\Big] \Big\}.\end{aligned}$$

Here, for a step-function density profile, r_b^2 depends on λ_b through the force-balance constraint $r_b^2(\lambda_b) = R_\lambda^2 + (R_\lambda^4 + 4R_\epsilon^4)^{1/2}$, where $R_\lambda^2 = \lambda_b e_b^2 / m_b \omega_{\beta\perp}^2$ and $R_\epsilon^2 = \tilde{\epsilon}/2\omega_{\beta\perp}$.

Evaluation of $\langle E_z^s \rangle^{(2)}$ for Step-Function Density Profile

- For step-function density profile, $\langle E_z^s \rangle^{(2)}$ can generally be expressed as

$$\langle E_z^s \rangle^{(2)} = -e_b r_w^2 \{ \tilde{g}_2 \frac{\partial^3 \lambda_b}{\partial z^3} + \tilde{g}_3 (\frac{\partial \lambda_b}{\partial z})^3 + \tilde{g}_4 \frac{\partial \lambda_b}{\partial z} \frac{\partial^2 \lambda_b}{\partial z^2} \},$$

  where the coefficients $\tilde{g}_2$, $\tilde{g}_3$ and $\tilde{g}_4$ depend on λ_b, $\partial r_b^2 / \partial \lambda_b$, etc.

- In the limit of a low-intensity beam ($R_\lambda^2 \ll 2R_\epsilon^2$), where $r_b^2 \simeq 2R_\epsilon^2 = const.$ (independent of λ_b), we obtain the expected result

$$\tilde{g}_2 = g_2 \ , \quad \tilde{g}_3 = 0 \ , \quad \tilde{g}_4 = 0 \ .$$

- For a high-intensity, space-charge dominated beam ($R_\lambda^2 \gg 2R_\epsilon^2$), it follows that $r_b^2 \simeq 2R_\lambda^2$, and the coefficients $\tilde{g}_2$, $\tilde{g}_3$ and $\tilde{g}_4$ can be approximated by

$$\tilde{g}_2 = \frac{1}{8}[4(1 - \frac{r_b^2}{r_w^2}) - 3\frac{r_b^2}{r_w^2} \ell n(\frac{r_w^2}{r_b^2})], \quad \tilde{g}_3 = \frac{r_b^2}{8\lambda_b^2 r_w^2}$$

$$\tilde{g}_4 = -\frac{3r_b^2}{8\lambda_b r_w^2}[1 + 2\ell n(\frac{r_w^2}{r_b^2})].$$

- These results clearly display the strong dependence of $\langle E_z^s \rangle^{(2)}$ on line density λ_b.

Longitudinal Vlasov-Maxwell Equations for Low Beam Intensity

- We specialize to the low-intensity regime ($R_\lambda^2 \ll 2R_\epsilon^2$) where the dependence of the beam radius r_b on line density λ_b can be neglected. In this case, the Vlasov-Maxwell equations describing the evolution of the longitudinal beam distribution $F_b(z, p_z, t)$ and line density $\lambda_b(z, t)$ can be expressed as

$$\frac{\partial F_b}{\partial t} + v_z \frac{\partial F_b}{\partial z} + e_b \langle E_z^s \rangle \frac{\partial F_b}{\partial p_z} = 0,$$

where

$$e_b \langle E_z^s \rangle = -e_b^2 g_0 \frac{\partial \lambda_b}{\partial z} - e_b^2 g_2 r_w^2 \frac{\partial^3 \lambda_b}{\partial z^3}.$$

- Here, the geometric factors g_0 and g_2 are defined by

$$g_0 = \ell n\left(\frac{r_w^2}{r_b^2}\right) + \alpha_n,$$

$$g_2 = \frac{1}{2}\left[1 - (1 - \beta_n)\frac{r_b^2}{r_w^2} - \frac{1}{n+2}\frac{r_b^2}{r_w^2}\ell n\left(\frac{r_w^2}{r_b^2}\right)\right].$$

Table of Values of g_0 and g_2

Profile Index n	Normalized Profile $(0 \le r < r_b)$ $\frac{\pi r_b^2 n_b}{\lambda_b} = (n+1)\left(1-\frac{r^2}{r_b^2}\right)^n$	Geometric Factor $g_0 = \ln\left(\frac{r_w^2}{r_b^2}\right) + \alpha_n$	Geometric Factor $g_2 = \frac{1}{2}\left[1-(1-\beta_n)\frac{r_b^2}{r_w^2} - \frac{1}{n+2}\frac{r_b^2}{r_w^2}\ln\left(\frac{r_w^2}{r_b^2}\right)\right]$
0	1	$\ln\left(\frac{r_w^2}{r_b^2}\right) + \frac{1}{2}$	$\frac{1}{2}\left[1-\frac{5}{6}\frac{r_b^2}{r_w^2} - \frac{1}{2}\frac{r_b^2}{r_w^2}\ln\left(\frac{r_w^2}{r_b^2}\right)\right]$
1	$2\left(1-\frac{r_w^2}{r_b^2}\right)$	$\ln\left(\frac{r_w^2}{r_b^2}\right) + \frac{11}{12}$	$\frac{1}{2}\left[1-\frac{41}{60}\frac{r_b^2}{r_w^2} - \frac{1}{3}\frac{r_b^2}{r_w^2}\ln\left(\frac{r_w^2}{r_b^2}\right)\right]$
2	$3\left(1-\frac{r_w^2}{r_b^2}\right)^2$	$\ln\left(\frac{r_w^2}{r_b^2}\right) + \frac{73}{60}$	$\frac{1}{2}\left[1-\frac{61}{105}\frac{r_b^2}{r_w^2} - \frac{1}{4}\frac{r_b^2}{r_w^2}\ln\left(\frac{r_w^2}{r_b^2}\right)\right]$
3	$4\left(1-\frac{r_w^2}{r_b^2}\right)^3$	$\ln\left(\frac{r_w^2}{r_b^2}\right) + \frac{1217}{840}$	$\frac{1}{2}\left[1-\frac{1279}{2520}\frac{r_b^2}{r_w^2} - \frac{1}{5}\frac{r_b^2}{r_w^2}\ln\left(\frac{r_w^2}{r_b^2}\right)\right]$
∞	$\frac{r_b^2}{R_b^2}\exp(-\frac{r^2}{R_b^2})$	$\ln\left(\frac{r_w^2}{2R_b^2}\right) + \gamma$	$\frac{1}{2}\left[1-(1+\gamma)\frac{R_b^2}{r_w^2} - \frac{R_b^2}{r_w^2}\ln\left(\frac{r_w^2}{2R_b^2}\right)\right]$

Values of the geometric factors g_0 and g_2 for several density profile shapes and low beam intensity ($R_\lambda^2 \ll 2R_\epsilon^2$). Here, $\gamma = 0.5772$ is Euler's constant.

Linearized Vlasov-Maxwell Equations for Low Beam Intensity

- Perturbations are taken to be of the form

$$\delta\psi(z,t) = \delta\widehat{\psi}\exp(ik_z z - i\omega t),$$

where k_z is the axial wavenumber, and ω is the complex oscillation frequency, with $Im\omega > 0$ corresponding to instability (temporal growth).

- The linearized Vlasov equation gives

$$\delta F_b = -k_z(e_b^2 g_0 - e_b^2 g_2 k_z^2 r_w^2)\frac{\partial F_b^0/\partial p_z}{\omega - k_z v_z}\delta\lambda_b,$$

which relates the perturbed distribution function δF_b to the perturbed line density $\delta\lambda_b$. We introduce effective sound speeds u_{b0} and u_{b2} associated with the geometric factors g_0 and g_1 defined by

$$u_{b0}^2 = \frac{g_0 e_b^2 \lambda_{b0}}{m_b}\ , \quad u_{b2}^2 = \frac{g_2 e_b^2 \lambda_{b0}}{m_b}.$$

The dispersion relation then becoms

$$D(k_z,\omega) = 0,$$

where the dielectric function $D(k_z,\omega)$ is defined by

$$D(k_z,\omega) = 1 + k_z(u_{b0}^2 - k_z^2 r_w^2 u_{b2}^2)\frac{m_b}{\lambda_{b0}}\int_{-\infty}^{\infty} dp_z \frac{\partial F_b^0/\partial p_z}{\omega - k_z v_z}.$$

Dispersion Relation for Low Beam Intensity

- Introducing the distribution function $f_b^0(p_z) \equiv \lambda_{b0}^{-1} F_b^0(p_z)$ normalized according to $\int_{-\infty}^{\infty} dp_z f_b^0(p_z) = 1$, and integrating by parts with respect to p_z using $\partial v_z/\partial p_z = 1/m_b$, the dispersion relation $D(k_z, \omega) = 0$ is readily expressed in the compact form

$$D(k_z, \omega) = 1 - k_z^2(u_{b0}^2 - k_z^2 r_w^2 u_{b2}^2) \int_{-\infty}^{\infty} \frac{dp_z f_b^0(p_z)}{(\omega - k_z v_z)^2} = 0.$$

- The dispersion relation can be used to calculate the complex oscillation frequency ω for a wide range of choices of beam distribution function $f_b^0(p_z)$. It is convenient to introduce the effective susceptibility $\chi(k_z, \omega)$ with dimensions (frequency)$^{-2}$ defined by

$$\chi(k_z, \omega) = \int_{-\infty}^{\infty} \frac{dp_z f_b^0(p_z)}{(\omega - k_z v_z)^2}.$$

  The resulting expressions for $\chi(k_z, \omega)$ are displayed in Table 2 for various choices of distribution function $f_b^0(p_z)$ ranging from a cold distribution function (Entry #1) to a Maxwellian distribution (Entry #5).

Table of Susceptibilities

Entry Number	Distribution $f_b^0(p_z)$	Susceptibility $\chi(k_z,\omega)$
1	$\delta(p_z)$	$\frac{1}{\omega^2}$
2	$f_b^0 = \begin{cases} \frac{1}{2m_b v_T}, & \lvert p_z\rvert < m_b v_T \\ 0, & \lvert p_z\rvert > m_b v_T \end{cases}$	$\frac{1}{(\omega^2 - k_z^2 v_T^2)}$
3	$\frac{m_b v_T}{\pi}\frac{1}{p_z^2+m_b^2 v_T^2}$	$\frac{1}{(\omega+i\lvert k_z\rvert v_T)^2}$
4	$\frac{2(m_b v_T)^2}{\pi}\frac{1}{(p_z^2+m_b^2 v_T^2)^2}$	$\frac{1}{(\omega+i\lvert k_z\rvert v_T)^2}\left[1+\frac{2i\lvert k_z\rvert v_T}{\omega+i\lvert k_z\rvert v_T}\right]$
5	$\frac{1}{m_b v_T}\exp\left(-\frac{p_z^2}{m_b^2 v_T^2}\right)$	$-\frac{2}{k_z^2 v_T^2}\left[1+\xi Z(\xi)\right]$

Susceptibility $\chi(k_z,\omega)$ for various choices of $f_b^0(p_z)$.

Example Corrsponding to Damped Sound Wave

- As a simple example, consider the Lorentzian distribution in Entry #3 of Table II. Substituting the expression for $\chi(k_z, \omega)$, we obtain the dispersion relation

$$(\omega + i|k_z|u_T)^2 = k_z^2(u_{b0}^2 - k_z^2 r_w^2 u_{b2}^2).$$

- The solutions for $k_z^2 r_w^2 \ll 1$ can be expressed as

$$Re\omega = \omega_r = \pm k_z u_{b0}\big(1 - \frac{1}{2}k_z^2 r_w^2 \frac{u_{b2}^2}{u_{b0}^2}\big) \ ,$$

$$Im\omega = \omega_i = -|k_z|u_T.$$

- Because $Im\omega = -|k_z|u_T < 0$, note that the wave perturbation is damped due to resonant wave-particle interactions (classical Landau damping) for the choice of Lorentzian distribution function in Table II.

Conclusions

- Self-consistent nonlinear kinetic model describing longitudinal beam dynamics has been developed for $k_z^2 r_w^2 < 1$ and arbitrary beam intensity.
- Average longitudinal field $\langle E_z^s \rangle$ exhibits a strong dependence on line density λ_b and shape of transverse density profile n_b.
- Collective excitations have been explored at low beam intensity.
- Further analysis of collective excitations at high beam intensity is required.

Background and References

[1] Allen, N, Brown and M. Reiser, Part. Accel. **45**, 149 (1994).

[2] W. M. Sharp, A. Friedman and D. P. Grote, Fusion Engineering and Design **32**, 201 (1996).

[3] R. C. Davidson and E. A. Startsev, Phys. Rev. ST Accel. Beams **7**, 024401 (2004).

[4] R. C. Davidson, Phys. Rev. ST Accel. Beams **7**, 054402 (2004).